Pseudoerror Monitor for 16 QAM 140 Mbit/s Digital Radio

RAMON AGUSTI, MEMBER, IEEE, AND FERNANDO CASADEVALL

Abstract—**This paper presents the performance of a pseudoerror monitoring technique for a 16 QAM 140 Mbit/s digital radio in presence of multipath dispersive fading. The so-called pseudoerrors, generated by means of a threshold modification of two, namely, secondary receivers are entered into an extrapolating function to obtain a fast bit error ratio (BER) calculation. A counting time of 10 ms was retained in order to follow fading depth changes up to 100 dB/s and fading notch speeds up to 300 MHz/s approximately. We have considered three structures for the receiver: without equalization, with IF amplitude equalization, and decision feedback equalization (DFE). The results obtained show the estimated and real BER within a margin that includes the two recommended CCIR values: 10^{-3} and 10^{-6}. In particular, the estimated signature obtained in the case of using IF equalization reveals that this fast BER calculation could be an effective choice to control a frequency diversity switch, even in the presence of a fading activity with rapid variations.**

I. Introduction

GENERALLY, digital radio systems are characterized by a low error ratio when operating within a broad range of noise and channel distortion values, followed by an abrupt drop in performance when a small increase in these values occurs. This causes problems in performance assessments when compared with analog transmission. In particular, low error ratio is difficult to monitor and its gradual degradation has no noticeable effect until, quite suddenly, errors are excessive.

It is widely accepted that a pseudoerror monitoring technique [1] is a powerful measurement strategy of data error rate in digital radio. It seems to overcome the drawbacks inherent either to the long measurement time of other in-service techniques or to the problems related to off-service monitoring. Moreover, it works with the unknown data stream of the customer and it does not require suitable test patterns. The philosophy of pseudoerror technique may be presented through the scheme of Fig. 1. A number of secondary receivers are connected in parallel to the main receiver prior to the detection circuits. These receivers are degraded by a known amount so as to generate the so-called pseudoerrors. Entering this amount of pseudoerrors into an extrapolating function, an estimate of the actual BER is obtained.

In the last years several works have appeared in order to assess the performance of pseudoerror monitoring (PEM) in the presence of flat fading [2] or with a controlled amount of amplitude or phase distortion [3]. However, little effort has been made to introduce the selective fading channel which most influences high capacity radio links [4]. In this paper we have characterized the selective fading by a Rummler model [5] and we have analyzed a PEM to operate in a 16 QAM 140 Mbit/s digital radio. In particular, the following receiver structures have been considered:

- receiver without any equalization protection
- receiver with amplitude IF equalizer and both minimum phase (MP) and nonminimum phase (NMP) fading
- receiver with a zero forcing nonlinear equalizer and both MP and NMP fading.

Moreover, we have envisaged how to take advantage of the fast BER calculation in order to control a frequency diversity switch that could provide a large reduction in digital radio outage time [6].

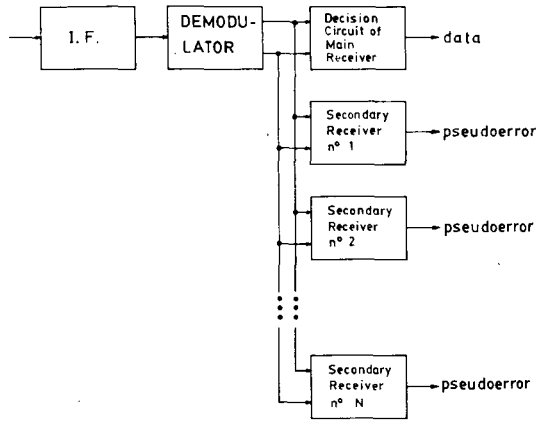

Fig. 1. Pseudoerror monitor scheme.

II. Shifted Threshold Error Monitor for 16 QAM Receivers

The pseudoerror monitor (PEM) chosen for 16 QAM digital radio links is based on a shifted threshold detection. Each secondary receiver is modified so as to create pseudoerror regions of decision, as shown in Fig. 2 by the shaded bands in the 16 QAM signal space. When a sample of the baseband demodulated signal falls on a pseudoerror region, a called pseudoerror will appear in the PEM output. The parameter that controls the amount of pseudoerrors generated is given by the threshold shift ΔS, whose value is the same for both the in-phase channel and the quadrature channel.

As we will see later in Section III, a true error ratio estimation may be performed by a linear extrapolation based on any couple of measured pseudoerror ratios. So, a pair of secondary receivers is to be retained in our approach.

Fig. 3 shows a low-pass equivalent model of the transmission system. The transmitted signal $s(t)$ can be formulated by

$$s(t)=\sum_{k=-\infty}^{\infty}(a_k+jb_k)\delta(t-kT) \qquad (1)$$

where a_k and b_k are two independent random variables which can take the values -3, -1, 1, 3 with the same probability.

Paper approved by the Editor for Radio Communication of the IEEE Communications Society. Manuscript received May 31, 1985; revised November 12, 1985.

The authors are with the Escuela Técnica Superior de Ingenieros de Telecomunicación de Barcelona (E.T.S.I.T.), APDO 30.002, 08071 Barcelona, Spain.

IEEE Log Number 8607999.

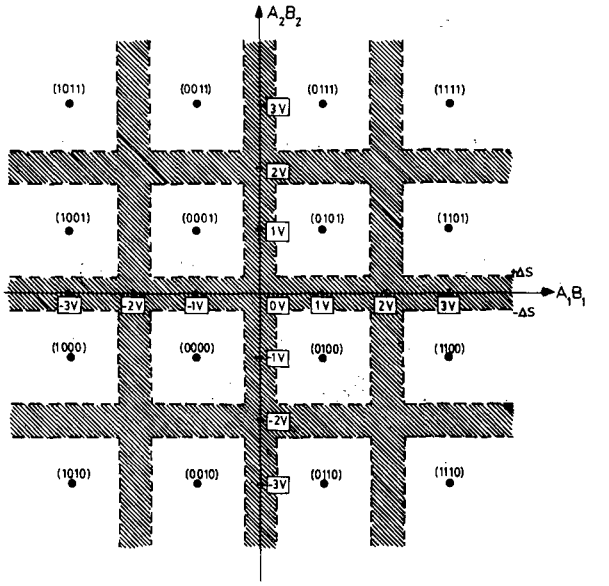

Fig. 2. 16 QAM space signal. The shaded areas represent the pseudoerror regions.

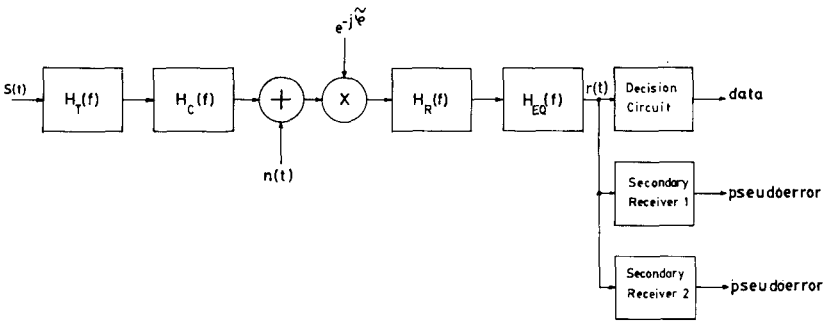

Fig. 3. Low-pass equivalent model of the transmission system.

Moreover, a_k and a_l, b_k and b_l are independent $\forall k \neq l$. Each value of a_k (resp. b_k) is associated with a state of the dibit (A_1, B_1) [resp. (A_2, B_2)], where A_1, B_1, A_2, B_2 are binary data to be transmitted. We assume a Gray encoding so that the two binary dibits associated with two consecutive values of a_k (resp. b_k) differ only by one bit [7]. A diagram of the encoded 16 QAM modulation can be seen in Fig. 2. Each level corresponds to the four bit words (A_1, B_1, A_2, B_2).

$H_T(f)$ is the low-pass equivalent function of all the transmitter filtering, $H_R(f)$ applies identically to the receiver filtering, and $H_C(f)$ introduces the presence of selective fading in the radio link. This transfer function is formulated by means of the Rummler model [5]:

$$H_C(f) = a[1 - be^{\pm j2\pi(f-fd)\tau}] \tag{2}$$

where a and b control the scale and shape of the fade, respectively, $A = -20 \log_{10}(1 - b)$ is the fading depth, $\tau = 6.3$ ns, fd is the frequency separation between the carrier and the fade minimum frequencies, and the plus and minus signs in the exponent correspond to NMP and MP fading, respectively.

$\tilde{\varphi}$ is introduced to model the real behavior of a carrier recovery loop. In our case we have considered a Costas recovery loop as representative; then [8]

$$\tilde{\varphi} = \frac{1}{4} \arg \int_{-\infty}^{\infty} h_f^4(u)\, du \tag{3}$$

$$h_f(t) = F^{-1}[H_T(f) \cdot H_C(f) \cdot H_R(f)]$$

where F^{-1} denotes inverse Fourier transform. The phase jitter introduced in the loop has not been taken into account.

$H_T(f)$ and $H_R(f)$ have been chosen to be raised cosine filtering when $H_C(f) = 1$; then

$$H_T(f) = H_R(f)$$

and

$$F^{-1}[H_T(f) \cdot H_R(f)] = \frac{\sin \pi \frac{t}{T}}{\pi \frac{t}{T}} \frac{\cos \beta\pi \frac{t}{T}}{1 - 4\beta^2 \frac{t^2}{T^2}} \tag{4}$$

where β is the rolloff factor.

Two types of equalizer structures have been basically proposed to compensate for the linear distortion: intermediate frequency equalization (IFE) and baseband equalization (BBE). IFE acts in the frequency domain in order to produce either an amplitude distortion or an amplitude and phase distortion complementary to that occurring in the channel. Two idealized configurations that maintain the basic features of the IFE have been analyzed.

a) MP Fading and Amplitude Equalization: This situation relies on the fact that real amplitude equalizers have a nonminimum phase structure for reasons of practical feasibility. Then, they will compensate in some degree the negative group delay of the distorted channel. In our case a pessimistic situation with an ideal amplitude equalization and without any

compensation for the group delay has been analyzed. Hence, the transfer function of the equalizer in Fig. 3 is given by

$$H_{EQ}(f)=\frac{1}{|H_C(f)|}\,.$$

b) NMP Fading and Amplitude Equalization: In this case we have considered the pessimistic situation of having an amplitude equalizer that compensates for both amplitude and phase in the MP case. Then with an NMP fading, this equalizer degrates the group delay of the channel by doubling it. So

$$H_{EQ}(f)=\frac{H_C(f)}{|H_C(f)|^2}\,.$$

BBE acts in the time domain to reduce intersymbol interference and crosstalk in the decision instants. Due to their known advantages, we have retained in our analysis a decision feedback equalizer, DFE [9].

Finally, $n(t)$ is a Gaussian complex noise with phase and quadrature components uncorrelated.

III. Pseudoerror and Error Rate Calculation

The receiver signal $r(t)$ can be expressed by

$$r(t)=\sum_{k=-\infty}^{\infty}[a_kP(t-KT)-b_kQ(t-KT)]$$

$$+j\sum_{k=-\infty}^{\infty}[b_kP(t-KT)+a_kQ(t-KT)]+u(t)+jv(t) \quad (5)$$

where, in general,

$$P(t)+jQ(t)$$

$$=F^{-1}\{[H_T(f)\cdot H_C(f)\cdot H_R(f)\cdot H_{EQ}(f)]\cdot e^{-j\tilde{\varphi}}\}. \quad (6)$$

$u(t)$ and $v(t)$ are the in-phase and quadrature received noise components, respectively. When selective fading is present, $P(t)$ differs from the Nyquist pulse, and thus, intersymbol interference appears. Moreover, if $Q(t)\neq 0$, crosstalk between the in-phase and quadrature data stream causes an additional degradation of the performance.

In order to compute the pseudoerror rate, we start by defining the pseudoerror regions when either A_1 or B_1 is transmitted. If $A_1 = 1$ is transmitted, one error in the main receiver is committed when the receiver signal sampling falls between $-2V$ and $2V$ in Fig. 2. (When $A_1 = 0$ is transmitted the contrary happens.) So, the corresponding pseudoerror regions are the two bands shown in Fig. 4 centered on $-2V$ and $2V$, respectively. Analogously, if $B_1 = 1$ is transmitted, an error in the main receiver is present when the received signal sampling is lower than zero. (When $B_1 = 0$ is transmitted the contrary happens.) So, the corresponding pseudoerror region is the middle band shown in Fig. 4. Things happen in a similar way when A_2 and B_2 are transmitted. To consider this situation, Fig. 4 should be rotated 90°.

We denote the in-phase and quadrature components of the complex receiver signal as $r_x(t)$ and $r_y(t)$, respectively; then

$$r(t)=r_x(t)+jr_y(t) \quad (7)$$

where

$$r_x(t_0)=G\left[a_0P_0(t_0)+\sum_{k\neq 0}a_kP_k(t_0)-\sum_k b_kQ_k(t_0)+u(t_0)\right]$$

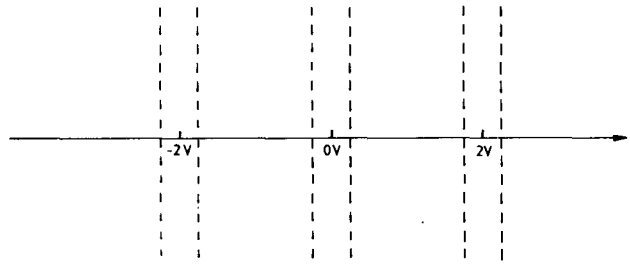

Fig. 4. In-phase pseudoerror region.

$$r_y(t_0)=G\left[b_0P_0(t_0)+\sum_{k\neq 0}b_kP_k(t_0)+\sum_k a_kQ_k(t_0)+v(t_0)\right]$$

$$P_k(t)=P(t-kT)$$

$$Q_k(t)=Q(t-kT)$$

and $\{t_0 + kT\}$ are the sampling instants.

G is a gain factor introduced to consider the presence of automatic gain control (AGC). Moreover, as $r_x(t)$ and $r_y(t)$ are statistically identical, only $r_x(t)$ will be considered. Equation (7) can be arranged as

$$r_x(t_0)=G[a_0P_0(t_0)+u(t_0)]+\alpha \quad (8)$$

where we have introduced the random variable α defined by

$$\alpha=G\left[\sum_{k\neq 0}a_kP_k(t_0)-\sum_k b_kQ_k(t_0)\right]\,. \quad (9)$$

Then, the A_1 pseudoerror rate is formulated by

$$P_{P,A_1}(\epsilon)=E_\alpha\{\text{Prob}\ [-2-\Delta S\leqslant r_x(t_0)\leqslant -2+\Delta S]$$

$$+\text{Prob}\ [2-\Delta S\leqslant r_x(t_0)\leqslant 2+\Delta S]\} \quad (10)$$

and $E_\alpha(\cdot)$ denotes the statistic mean with respect to the random variable α.

After some algebraic effort, we obtain

$$P_{P,A_1}(\epsilon)=\frac{1}{4}E_\alpha\{\text{erfc}\ [1-\Delta S+\alpha+3(GP_0-1))\rho_0]$$

$$+\text{erfc}\ [(1-\Delta S+\alpha-(GP_0-1))\rho_0]$$

$$-\text{erfc}\ [(1+\Delta S+\alpha+3(GP_0-1))\rho_0]$$

$$-\text{erfc}\ [(1+\Delta S+\alpha-(GP_0-1))\rho_0]\} \quad (11)$$

where $\rho_0 = \sqrt{\eta/10}$ and η is the mean value of the signal-to-noise ratio at the input of the decision circuit.

In an analogous way, we have

$$P_{P,B_1}(\epsilon)=E_\alpha\{\text{Prob}\ [-\Delta S\leqslant r_x(t_0)\leqslant \Delta S]\}. \quad (12)$$

Operating, we obtain

$$P_{P,B_1}(\epsilon)=\frac{1}{4}E_\alpha\{\text{erfc}\ [1-\Delta S+\alpha+(GP_0-1))\rho_0]$$

$$-\text{erfc}\ [(1+\Delta S+\alpha(GP_0-1))\rho_0]\}. \quad (13)$$

Finally, the bit pseudoerror ratio probability is calculated as

$$P_P(\epsilon)=\frac{1}{4}P_{P,A_1}(\epsilon)+\frac{1}{4}P_{P,B_1}(\epsilon)+\frac{1}{4}P_{P,A_2}(\epsilon)+\frac{1}{4}P_{P,B_2}(\epsilon). \quad (14)$$

As $P_{P,A_1}(\epsilon) = P_{P,A_2}(\epsilon)$, $P_{P,B_1}(\epsilon) = P_{P,B_2}(\epsilon)$, by substituting

$P_{P,A_1}(\epsilon)$, $P_{P,B_1}(\epsilon)$ in the above formula, we have

$$P_p(\epsilon)=\int_{\infty}^{\infty} P_1(x)f_\alpha(x)\ dx \tag{15}$$

where

$$\begin{aligned}P_1(x)=\frac{1}{8}\{&\text{erfc}\ [(1-\Delta S+x+3(GP_0-1))\rho_0]\\&+\text{erfc}\ [(1-\Delta S+x-(GP_0-1))\rho_0]\\&+\text{erfc}\ [(1-\Delta S+x+(GP_0-1))\rho_0]\\&-\text{erfc}\ [(1+\Delta S+x+3(GP_0-1))\rho_0]\\&-\text{erfc}\ [(1+\Delta S+x-(GP_0-1))\rho_0]\\&-\text{erfc}\ [(1+\Delta S+x+(GP_0-1))\rho_0]\}\end{aligned}$$

and $f_\alpha(x)$ is the probability density function of the random variable α.

The calculation of $P_P(\epsilon)$ in (15) has been based on the Gaussian quadrature rule (GQR) [10]. This is an exact method that requires only a few moments of the random variable α to assure a fast convergence. In that case, the expression (15) can be computed as

$$P_p(\epsilon)=\sum_{i=1}^{N} w_iP_1(x_i). \tag{16}$$

The x_i are called the abscissas of the formula and the w_i the weights, so the set $\{w_i, x_i\}_{i=1}^{N}$ is called a quadrature rule corresponding to the weight function $f_\alpha(x)$.

To validate the PEM operation, an error ratio calculation of the main receiver is needed. In this case it is found after some algebraic effort:

$$\begin{aligned}P_e(\epsilon)=E_\alpha\Bigg[\frac{1}{8}\{&\text{erfc}\ [(1+\alpha+3(GP_0-1))\rho_0]\\&+\text{erfc}\ [(1+\alpha-(GP_0-1))\rho_0]\\&+\text{erfc}\ [(1+\alpha+(GP_0-1))\rho_0]\}\Bigg].\end{aligned} \tag{17}$$

IV. Pseudoerror and Error Rates Relationship

In a 16 QAM system without distortion, $G = 1$ and $\alpha = 0$, the pseudoerror and error rates are calculated from (15) and (17) as

$$\begin{aligned}P_p(\epsilon)&\cong\frac{3}{8}\left\{\text{erfc}\left(\sqrt{\frac{(1-\Delta S)^2\eta}{10}}\right)\right.\\&\left.-\text{erfc}\left(\sqrt{\frac{(1+\Delta S)^2\eta}{10}}\right)\right\}\\&\simeq\frac{3}{8}\text{erfc}\left(\sqrt{\frac{(1-\Delta S)^2\eta}{10}}\right)\end{aligned} \tag{18}$$

and

$$P_e(\epsilon)\simeq\frac{3}{8}\text{erfc}\left(\sqrt{\frac{\eta}{10}}\right).$$

For $\eta \gg 1$, we have

$$P_p(\epsilon)\simeq\frac{3}{8\sqrt{2\pi}}\frac{\exp\ [-(1-\Delta S)^2\eta/10]}{\sqrt{(1-\Delta S)^2\eta/10}} \tag{19}$$

and

$$P_e(\epsilon)\simeq\frac{3}{8\sqrt{2\pi}}\frac{\exp\ (-\eta/10)}{\sqrt{\eta/10}}. \tag{20}$$

The approximately linear behavior of $\log P_e(\epsilon)$ and $\log P_P(\epsilon)$ can be used to set a linear relationship between both expressions [1]. Then

$$\log\ P_P(\epsilon)=K\cdot M+\log\ P_e(\epsilon). \tag{21}$$

By substituting (21) for (19) and (20), and operating in a similar way as in [3], we obtain

$$K=\frac{\eta}{10} \tag{22a}$$

$$M=\Delta S(2-\Delta S) \tag{22b}$$

where we have assumed

$$\frac{1}{2}\ln\left[(1-\Delta S)^2\frac{4\eta\pi}{10}\right]\simeq\frac{1}{2}\ln\left(\frac{4\eta\pi}{10}\right). \tag{23}$$

Now, by writing (21) as

$$P_P(\epsilon)=10^{K\cdot M}P_p(\epsilon)=G_PP_e(\epsilon), \tag{24}$$

the error ratio could be evaluated from the $P_{P,A_1}(\epsilon)$ by choosing a factor gain G_P for each η value. However, this process is too cumbersome and it is preferable to choose a unique G_P value within a wide range of η values. To carry out this procedure, a linear extrapolation of two pseudoerror ratios: $P_{P_1}(\epsilon)$ and $P_{P_2}(\epsilon)$, obtained from two secondary paths, with ΔS_1 and ΔS_2 as threshold shifts, can be used. Then, from the corresponding two equations

$$\log\ P_{P_i}(\epsilon)=K_iM_i+\log\ \hat{P}_e(\epsilon),\qquad i=1,\ 2 \tag{25}$$

we have

$$\log\ \hat{P}_e(\epsilon)=\frac{M_2\ \log\ P_{P_1}(\epsilon)-M_1\ \log\ P_{P_2}(\epsilon)}{M_2-M_1} \tag{26}$$

where

$$M_1=\Delta S_1(2-\Delta S_1)$$

$$M_2=\Delta S_2(2-\Delta S_2)$$

and $\hat{P}_e(\epsilon)$ is the estimated error rate.

V. Results and Discussion

A. Calculation Details

We have obtained results for a 16 QAM system working at 140 Mbits/s. The channel parameters considered are $\beta = 0.4$, $fdT = 0$, 0.4, 0.8 and 1.2, $a = 0.1$ (−20 dB) and SNR = 60 dB when $a = 1$, $b = 0$. The chosen "a" value is taken as representative because the selective fading activity is foreseen to appear most of the time in conjunction with 15 dB $< -20\cdot\log_{10}(a) <$ 25 dB [5]. On the other hand, because $P_e = 10^{-3}$ is obtained with SNR $\simeq$ 18 dB in an ideal 16 QAM system, the chosen SNR = 60 dB sets up a typical flat fade margin of 42 dB.

The computation of the $2N + 1$ moments, necessary to perform the GQR, has been accomplished by an exhaustive method considering a truncated impulse response of a $7T$ duration. A good convergence of the GQR algorithm has always been reached with $N \leqslant 6$. The sampling instant t_0 has been chosen according to the classical square-law envelope timing recovery [11].

The automatic gain control (AGC) retained works by comparing the actual received power to the expected power in an ideal situation, so

$$G=\frac{\int_{\infty}^{\infty}|H_T(f)\cdot H_R(f)|^2\,df}{\int_{\infty}^{\infty}|H_T(f)\cdot H_C(f)\cdot H_R(f)|^2\,df}; \tag{27}$$

The action of the AGC introduces a noise power increase given by

$$\Delta_1=10\ \log\ G.$$

An additional degradation of the SNR value arises due to the presence of IFE and BBE. When only IFE is introduced, the noise power increase is

$$\Delta_2=10\ \log\ \left[\int_{\infty}^{\infty}|H_{eq}(f)|^2\,df\right]. \tag{28}$$

When BBE is present, the corresponding noise power increase is [12]

$$\Delta_3=10\ \log\ \left[\sum_{j=-N}^{0}|C_j|^2\right] \tag{29}$$

where C_j is the value of the linear equalizer taps.

B. PEM Parameters

The pseudoerror ratio estimated, $\hat{P}_p$, can be obtained as the ratio of the number of counted pseudoerrors to the total number of transmitted bits in a sufficiently long time interval. Then

$$\hat{P}_p=\frac{N_P}{140\cdot 10^6\cdot t_c} \tag{30}$$

where N_P is the number of binary errors detected during the counting time t_c.

PEM parameters N_P, t_c, ΔS_1, and ΔS_2 are chosen depending on the accuracy required of the P_e estimation. A good $\hat{P}_P$ value can be obtained if $N_P > 10$. On the other hand, we are interested in monitoring the error rate even when exceptional rates of change in the fading activity arise. Hence, the counting time t_c should be kept as short as possible in order to monitor the system without an excessive variation on the received signal during the counting process. So, a $t_c = 10$ ms has been chosen to manage the exceptional rates of change actually registered of 100 dB/s and 300 MHz/s in the fading deep and fading notch position, respectively [13]. Then, variations in the received signal attenuation less than 1 dB and normalized frequency separation, fdT, less than 0.1 could be maintained during the mentioned counting process. This would allow a stationary analysis of the error ratio performance. Moreover, the t_c value can also meet the CCIR requirement of having a switching operation time less than 40 ms [14] if a PEM were used to control an automatic switch of a diversity digital radio system. This value is thus adopted to give an order of mangitude.

With $N_P = 10$ and $t_c = 10$ ms, the minimum $\hat{P}_P$ value would be $\hat{P}_P = 7.14\cdot 10^{-6}$. As the Recommendations [15] used in digital radio establish two BER values, namely 10^{-3} and 10^{-6}, we have chosen $P_e = 10^{-8}$ as the minimum value to be estimated. Then, the factor gain will be

$$G_P \geq \frac{7.14\cdot 10^{-6}}{10^{-8}}=714.$$

In particular, $G_{P_1} = 10^3$ and $G_{P_2} = 10^4$ have been retained in our approach with two secondary receivers. Substituting these values in (20) and (21), there results $\Delta S_1 = 0.284$, $M_1 = 0.488$, $\Delta S_2 = 0.405$, and $M_2 = 0.646$.

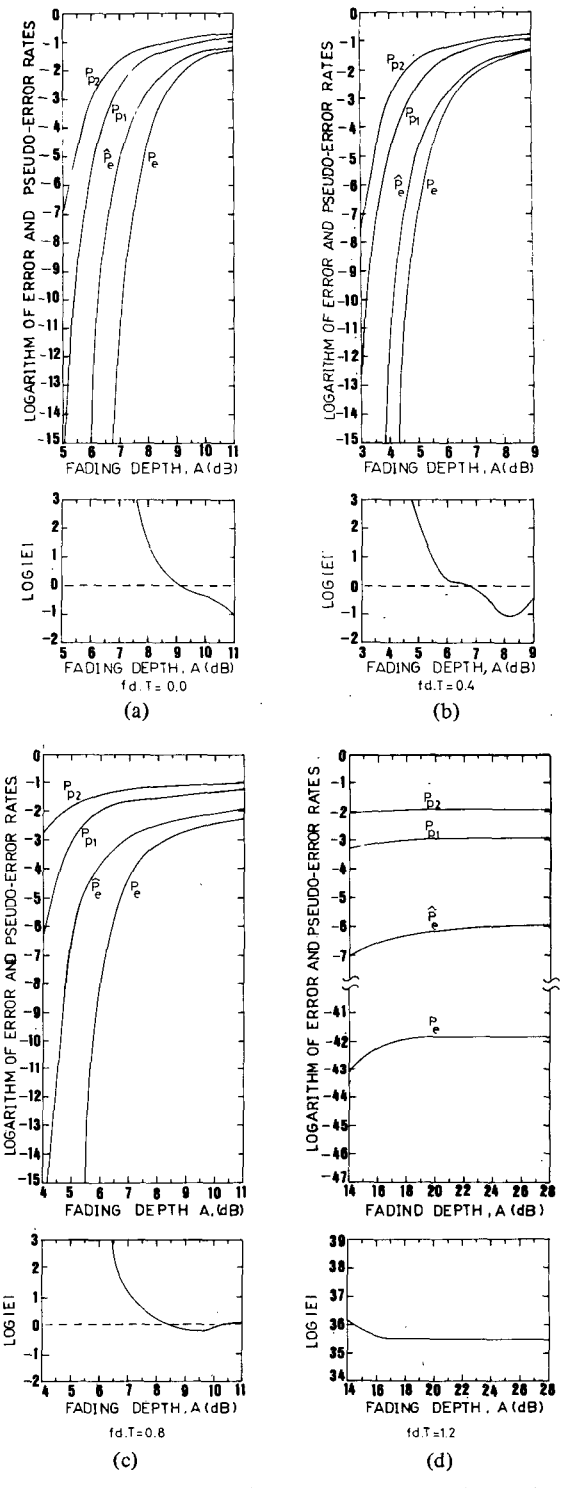

Fig. 5. Error and pseudoerror ratios as function of the fading depth, A, for an unequalized receiver. $\tau/T = 0.2205$, SNR = 60 dB.

Fig. 5 shows P_{P_1}, P_{P_2}, $\hat{P}_e$, and P_e versus the fading depth A, for the unequalized receiver. This figure also show the normalized estimation error defined as

$$|E|=\frac{[P_e-\hat{P}_e]}{\min\ \{P_e,\ \hat{P}_e\}}. \tag{31}$$

The $|E|$ value depends on the channel distortion and the SNR value. Specifically, a significant number of pseudoerrors can appear even when the eye diagram is open enough and noise is not present. It would be sufficient that the eye aperture were

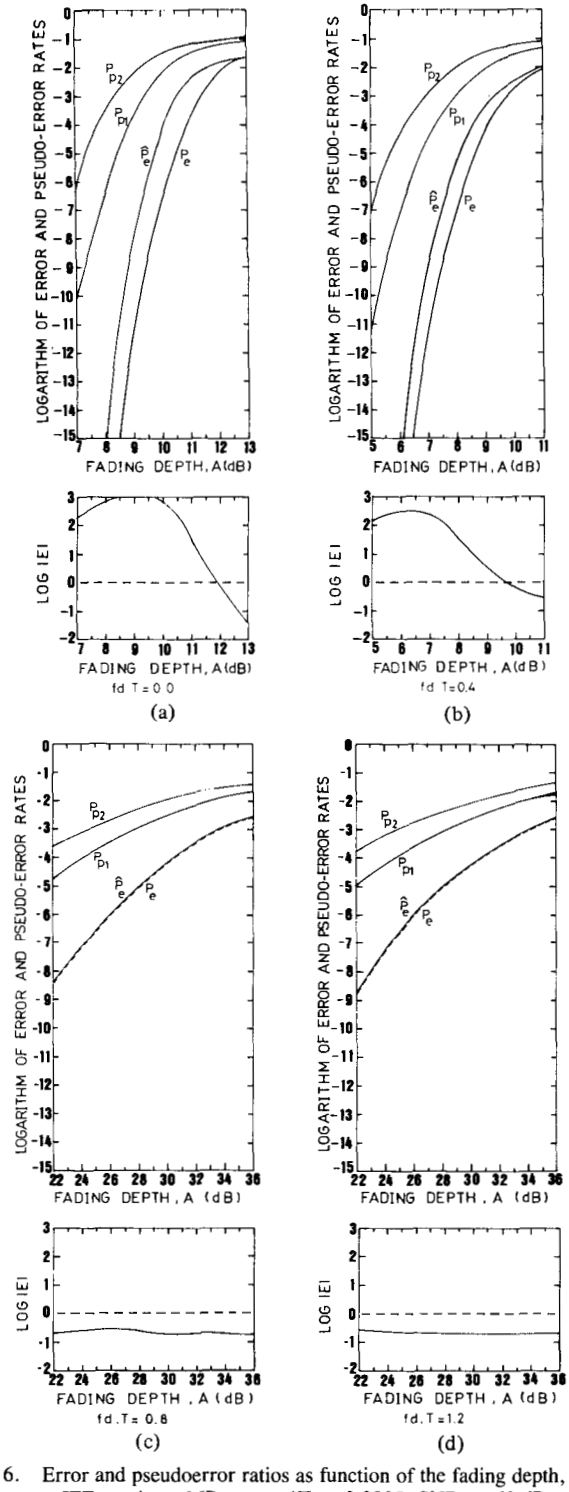

Fig. 6. Error and pseudoerror ratios as function of the fading depth, A, for an IFE receiver, MP case. $\tau/T = 0.2205$, SNR = 60 dB.

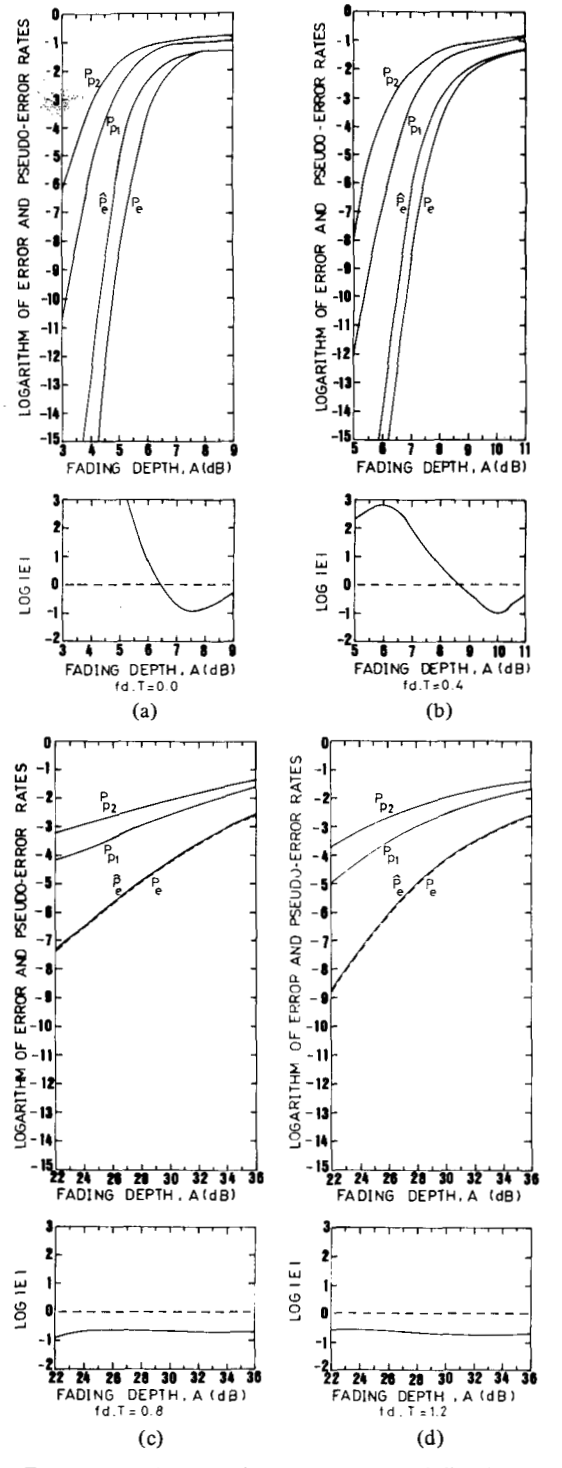

Fig. 7. Error and pseudoerror ratios as function of the fading depth A, for an IFE receiver, NMP case. $\tau/T = 0.2205$, SNR = 60 dB.

less than ΔS_2 and/or ΔS_1. In that case $|E| = \infty$. A similar situation appears in our case when the distortion is moderately high, for example, $fdT \simeq 1.2$ or $A \simeq 5$ dB. When the fading depth increases, the noise power increase Δ_1 becomes more relevant. Then, this noise can contribute appreciably to the total amount of pseudoerrors and the asymptotic pseudoerror and error ratio relationships, shown in Section IV, are most closely satisfied. This fact would explain the PEM performance improvement as the fading depth increases.

Fig. 6 shows the PEM performance in presence of MP fading and IFE. PEM results are also shown in Fig. 7 for NMP fading and IFE. Both MP and NMP fading present similar PEM performance for fdT lower than 0.6 approximately. In this case, group delay distortion dominates amplitude distortion. Consequently, the action of IFE is not significant and PEM performance is not far from the PEM performance shown above for the unequalized system. However, for $f_dT \gtrsim 0.6$, as amplitude distortion is the worst fading degradation effect, the IFE counteracts most channel distortion, noise becomes the first cause of degradation, and the PEM performs quite well.

Fig. 8 shows the estimate and real signatures in the cases

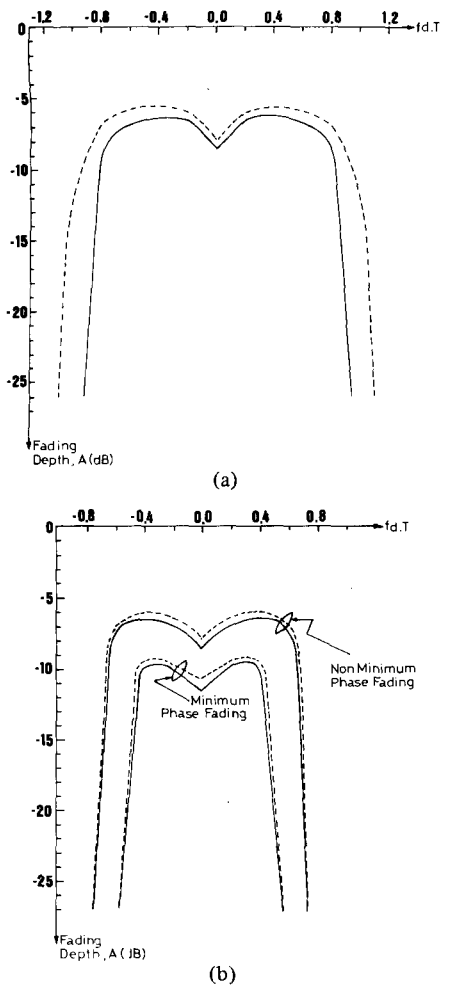

Fig. 8. Estimated signature (dashed line) and real signature (continuous line). τ/T = 0.2205, SNR = 60 dB. (a) Unequalized receiver. (b) IFE receiver.

analyzed above. It can be noticed that a switching diversity system controlled by the PEM should perform satisfactorily because the real signature is upper bounded by the estimated one. In particular, this is true when IFE is adopted. Then a 0.5 dB maximum fading depth error is appreciated, whichever fdT value is considered. In that case the PEM would perform as a fast error ratio estimator to take advantage of the large diversity improvement when a frequency diversity protection switch is adopted [6].

Fig. 9 shows the PEM performance for an MP fading in the presence of a DFE with two taps in the linear part and two taps in the nonlinear part. This structure seems to perform reasonably well in both MP and NMP fading cases [16]. As this equalizer almost completely eliminates the channel distortion, the estimated and the real error ratios practically coincide. An SNR = 50 dB has been chosen in order to present in Fig. 9 error ratio results ranging as in the above cases.

VI. Conclusion

A theoretical analysis of the shifted-threshold error rate monitor for a 16 QAM 140 Mbit/s digital radio in the presence of multipath dispersive fading has been carried out. Nonminimum and minimum phase fading and receiver structures such as unequalized receiver, IF amplitude equalizer, and baseband nonlinear equalizer have been analyzed. The obtained results allow us to assess the monitor performance for typical error rate values ranging from 10^{-3} to 10^{-6}. The use of this monitor as a fast technique for initiating the changeover operation of a frequency diversity switch has also been envisaged and its performance evaluated by means of the estimated signature. When used in conjunction with an IF amplitude equalizer, this protection switching initiator seems to be particularly effective.

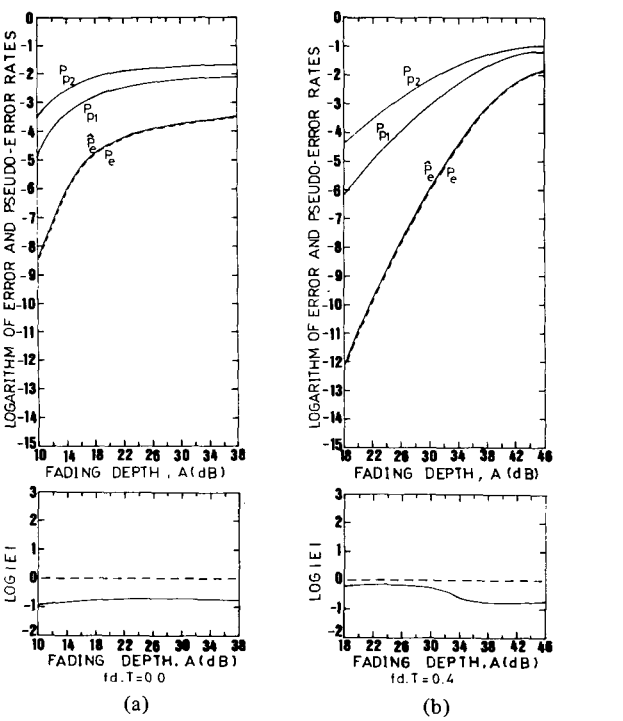

Fig. 9. Error and pseudoerror ratios as function of the fading depth, A, for a DFE receiver, MP case. τ/T = 0.2205, SNR = 50 dB.

References

[1] D. J. Gooding, "Performance monitor techniques for digital receivers based on extrapolation of error rate," *IEEE Trans. Commun. Technol.*, vol. COM-16, pp. 380–387, June 1968.

[2] M. Sant'Agostino, "Performance monitoring devices for digital radio-relay links," CSELT Rapporti i tecnici 4, Dec. 1975, pp. 13–29.

[3] E. A. Newcombe and S. Pasupathy, "Error rate monitoring in partial response system," *IEEE Trans. Commun.*, vol. COM-28, pp. 1052–1061, July 1980.

[4] CCIR Rep. 613-2, vol. IX-I, Geneva, Switzerland, 1982.

[5] W. D. Rummler, "A new selective fading model: Application to propagation data," *Bell Syst. Tech. J.*, vol. 58, pp. 1037–1071, May–June 1979.

[6] P. L. Dirner and S. H. Lin, "Measured frequency diversity improvement for digital radio," *IEEE Trans. Commun.*, vol. COM-33, pp. 106–109, Jan. 1985.

[7] P. Dupuis, M. Joindot, A. Leclert, and D. Soufflet, "16 QAM modulation for high capacity digital radio system," *IEEE Trans. Commun.*, vol. COM-27, pp. 1771–1782, Dec. 1979.

[8] R. Agustí, G. Junyent, and M. Joindot, "Etude du comportement d'une boucle de Costas en modulation MAQ 16 en présence d'évanuissements selectifs," *Ann. Télécommun.*, vol. 38, pp. 331–341, July–Aug. 1983.

[9] M. Joindot, A. Leclerc, J. Oudart, C. Rolland, and P. Vandamme, "Baseband adaptive equalization for a 16 QAM system in the presence of multipath propagation," in *Proc. Int. Conf. Commun.*, Denver, CO, 1981, paper 13.3.

[10] G. H. Golub and J. H. Welsch, "Calculation of Gauss quadrature rules," *Math. Comput.*, vol. 23, pp. 221–230, Apr. 1969.

[11] N. Amitay and L. J. Greenstein, "Multipath outage performance of digital radio receivers using finite-tap adaptive equalizers," *IEEE Trans. Commun.*, vol. COM-32, pp. 597–608, May 1984.

[12] A. P. Clark, *Advanced Data Transmission Systems.* London, England: Pentech, 1977, p. 212.

[13] L. Martin, "Rates of change of propagation medium transfer functions during selective fadings," in *Proc. URSI Commission F, 1983 Symp.*, Louvain, Belgium, June 1983.

[14] CCIR Rec. 477, vol. IX-I, Geneva, Switzerland, 1982.
[15] CCIR Rec. 594 (modified), Doc. 9/382-F, Geneva, Switzerland, 1985.
[16] H. Sari, "Baseband equalizer performance in the presence of selective fading," in *Proc. Globecom '83*, San Diego, CA, Nov. 28–Dec. 1, 1983, paper 1.1.

★

Ramon Agusti (M'78) was born in Riba-roja d'Ebre, Spain, on August 15, 1951. He received the Engineer of Telecommunications degree from the Universidad Politécnica de Madrid, Spain, in 1973, and the Ph.D. degree from the Universidad Politécnica de Catalunya, Spain, in 1978.

In 1973 he joined the Escuela Técnica Superior de Ingenieros de Telecomunicación de Barcelona, Spain, where he has been an Associate Professor since 1978. He has been working in the field of digital communications, with particular emphasis on digital radio and its performance under multipath propagation conditions. In the last few years he has also been concerned with the performance analysis and development of frequency-hopped spread-spectrum systems.

★

Fernando Casadevall was born in Barcelona, Spain, on April 22, 1955. He received the Engineer of Telecommunication and Ph.D. degrees from the Universidad Politécnica de Catalunya, Spain, in 1977 and 1983, respectively.

In 1978 he joined the Escuela Técnica Superior de Ingenieros de Telecomunicación de Barcelona, where he has been an Associate Professor since 1983. After graduation he was concerned with equalization techniques for digital fiber optic systems. His present research interests are in the areas of digital radio and spread-spectrum mobile communications.